PHYSICAL REVIEW E **75**, 045201(R) (2007)

Synthesizing folded band chaos

Ned J. Corron, Scott T. Hayes, Shawn D. Pethel, and Jonathan N. Blakely
U. S. Army RDECOM, AMSRD-AMR-WS-ST, Redstone Arsenal, Alabama 35898, USA
(Received 18 October 2006; published 12 April 2007)

A randomly driven linear filter that synthesizes Lorenz-like, reverse-time chaos is shown also to produce Rössler-like folded band wave forms when driven using a different encoding of the random source. The relationship between the topological entropy of the random source, dissipation in the linear filter, and the positive Lyapunov exponent for the reverse-time wave form is exposed. The two drive encodings are viewed as grammar restrictions on a more general encoding that produces a chaotic superset encompassing both the Lorenz butterfly and Rössler folded band paradigms of nonlinear dynamics.

DOI: 10.1103/PhysRevE.75.045201 PACS number(s): 05.45.Ac

Recently, it was shown that chaotic wave forms nearly identical to those of the famous Lorenz system can be synthesized via linear superposition of equally spaced but randomly polarized pulses [1–3]. Viewed in reverse time, this process admits a simple physical realization as a second-order linear filter driven by square waves of random sign [4]. Since this completely novel source of chaos lies outside the normal scope of nonlinear dynamics, it is important to consider what other topologically distinct chaotic dynamics can be synthesized. In this Rapid Communication we show that the same second-order linear filter that generates Lorenz-like butterfly dynamics in reverse time also produces Rössler-like folded band wave forms when driven by a different random signal. Moreover, the drive signals that yield these wave forms can be defined by grammar restrictions on a more general class of drive signals that produces a chaotic superset. Through these examples we elucidate a relationship between the determinism in the output wave form, the topological entropy of the drive signal, the dissipation in the linear filter, and the positive Lyapunov exponent for the reverse-time chaotic wave form.

To begin, we consider the second-order linear filter

$$\ddot{x} + 2\beta\dot{x} + (\omega^2 + \beta^2)x = (\omega^2 + \beta^2)s(t) \tag{1}$$

where $\omega=2\pi$, $\beta>0$ sets the dissipation, $s(t)$ is a random forcing, and $x(t)$ is the filter output. In Ref. [4], the dissipation is $\beta=\ln 2$ and the forcing is a random binary sequence $\{s_n\}$, where each bit is encoded by the polarity of a unit-length square pulse as shown in Fig. 1(a). In Fig. 2(a) we show a projection of the filter output using time-delay embedding. This wave form contains a Bernoulli shift dynamic and the "attractor" is topologically similar to the famous Lorenz butterfly attractor [5].

We now consider the filter (1) driven by a random binary sequence using the encoding shown in Fig. 1(b). As before, a bit $s_n=0$ encodes to low level for unit duration. However, now a bit $s_n=1$ encodes as high level for one-half time unit, followed by low level for a full unit. A projection of the resulting filter output for $\beta=\ln 2$ using this new encoding is shown in Fig. 2(b). In the following, we show that this wave form, when viewed in reverse time, is chaotic and topologically similar to Rössler's folded band attractor [6]. We also consider the effects of changing the filter parameter β and the identification of a critical, matched dissipation.

To begin, we examine the action of the filter for each possible encoded bit. Without loss of generality, we use $s(t)=1$ for the high level and $s(t)=0$ for the low level. Thus, for $s_n=0$ we have $s(t)=0$, and the general solution to Eq. (1) is

$$x(t) = Ae^{-\beta t}\sin(\omega t + \phi) \tag{2}$$

where A and ϕ are constants of integration. For a low-level signal of unit duration, this solution admits

$$x(t+1) = e^{-\beta}x(t). \tag{3}$$

For $s_n=1$, we first take $s(t)=1$, for which the general solution is

$$x(t) = 1 + Be^{-\beta t}\sin(\omega t + \theta) \tag{4}$$

where B and θ are constants of integration. For a high-level signal of one-half unit duration, the solution yields

$$x(t+1/2) = 1 + e^{-\beta/2}[1 - x(t)]. \tag{5}$$

The remainder of the encoding for $s_n=1$ again uses $s(t)=0$ for unit duration. Thus, Eqs. (3) and (5) combine to give

$$x(t+3/2) = e^{-\beta} + e^{-3\beta/2}[1 - x(t)]. \tag{6}$$

Defining the nth Poincaré return to coincide with the end of the encoded symbol s_n, we use Eqs. (3) and (6) to find that successive returns are related by

$$x_n = \begin{cases} e^{-\beta}x_{n-1}, & s_n = 0, \\ e^{-\beta} + e^{-3\beta/2}(1 - x_{n-1}), & s_n = 1, \end{cases} \tag{7}$$

where x_n is the value of the filter output at the nth return. It is straightforward to show that the iterated map (7) is closed

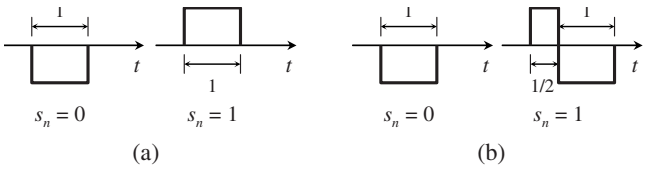

FIG. 1. Basis pulses for encoding a random sequence s_n and driving a linear filter to synthesize reverse-time chaos similar to (a) the Lorenz butterfly and (b) Rössler's simply folded band.

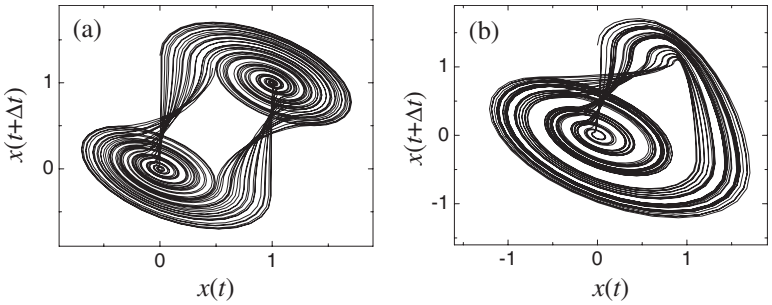

FIG. 2. Projection by time-delay embedding ($\Delta t=1/3$) of linear filter output wave form with $\beta=\ln 2$ using (a) the Lorenz-like butterfly encoding and (b) the Rössler-like folded band encoding.

on the interval $[0, e^{-3\beta/2}+e^{-\beta}]$ for any sequence $\{s_n\}$ and $\beta>0$.

We first consider the case of strong dissipation $\beta>\tilde{\beta}$, where $\tilde{\beta}$ is the unique real solution of

$$e^{-3\tilde{\beta}/2}+e^{-\tilde{\beta}}=1. \tag{8}$$

Analysis yields $\tilde{\beta}\cong 0.81\ln 2$, so this case includes the results shown in Fig. 2(b). For $0<x_{n-1}<1$, it is straightforward to show that $0<x_n<e^{-\beta}$ for $s_n=0$ and $e^{-\beta}<x_n<1$ for $s_n=1$. Thus, s_n is a function of x_n only, and we can invert the map (7) to get

$$x_{n-1}=\begin{cases} e^{\beta}x_n, & x_n<e^{-\beta}, \\ 1+e^{\beta/2}-e^{3\beta/2}x_n, & x_n>e^{-\beta}. \end{cases} \tag{9}$$

This reverse-time map is a piecewise-linear, skew-tent map as shown in Fig. 3(a), and the filter output exhibits dynamics consistent with this map. Since the slope of each linear segment in Eq. (9) is greater than 1, the reverse-time wave form is chaotic and characterized by a positive Lyapunov exponent ($\lambda=\beta$). Significantly, the unimodal map function implies that the reverse-time dynamics are characterized by a simply folded band similar to Rössler's attractor [6]. However, the map (9) has an escape region for $e^{-3\beta/2}+e^{-\beta}<x_n<1$, from which subsequent backward iterates grow without bound. As such, the backward map (9) is unstable and characterized by a chaotic transient [7]. A property of the chaotic transient is that there exists a Cantor set of initial conditions from which backward iterates do not enter the escape region and remain bounded: one of these atypical reverse-time trajectories describes any particular wave form observed from the linear filter. Consequently, the output filter wave form, when viewed in reverse time, is chaotic and evolves in this Cantor set.

For the case of weak dissipation $\beta<\tilde{\beta}$, we have that $e^{-\beta}+e^{-3\beta/2}>1$ and iterates x_n of the map (7) do not partition according to the drive symbol s_n. Thus the inverse of (7) must maintain x_n and s_n separately as

$$x_{n-1}=\begin{cases} e^{\beta}x_n, & s_n=0, \\ 1+e^{\beta/2}-e^{3\beta/2}x_n, & s_n=1. \end{cases} \tag{10}$$

This map is shown in Fig. 3(c). Although there is no escape region, x_{n-1} is now a multi-valued function of x_n, explicitly depending on s_n. In terms of the reverse-time dynamics, determinism is lost since the random sequence is required in addition to an initial condition to describe a reverse-time wave form. We make the conjecture that determinism can be regained by enforcing a grammar restriction on the random source, to which we return below.

For the critical dissipation $\beta=\tilde{\beta}$, we get a combination of the prior cases. First, we have that x_n determines s_n via the partition at $e^{-\beta}$ and the map (7) can be inverted per Eq. (9). This explicit dependence of x_{n-1} on just x_n implies determinism in the reverse-time wave form. Second, we find that iterates of the map (7) are closed on the interval $0\leqslant x_n\leqslant 1$ and there is no escape region for the backward map. Thus, the reverse-time map is stable and bounded. The map for this case is shown in Fig. 3(b). This skew-tent map exhibits chaotic dynamics and a positive Lyapunov exponent ($\lambda=\tilde{\beta}$). Since this map is a unimodal one-dimensional map, kneading theory can be used to show that the map represents a full shift and exhibits an unrestricted symbolic grammar [8]. A sample wave form produced by the filter for $\beta=\tilde{\beta}$ is shown in Fig. 4. Compared to Fig. 2(b), the embedding shown in Fig. 4(b) does not show any gaps and appears fully connected, confirming that trajectories are not restricted to a Cantor set. This chaotic set is topologically similar to Rössler's simply folded band attractor [6]. However, the structure in Fig. 4(b) differs in that it is two dimensional with no transverse thickness; thus, the reverse-time wave form is not invertible nor described by a flow. In contrast, the attrac-

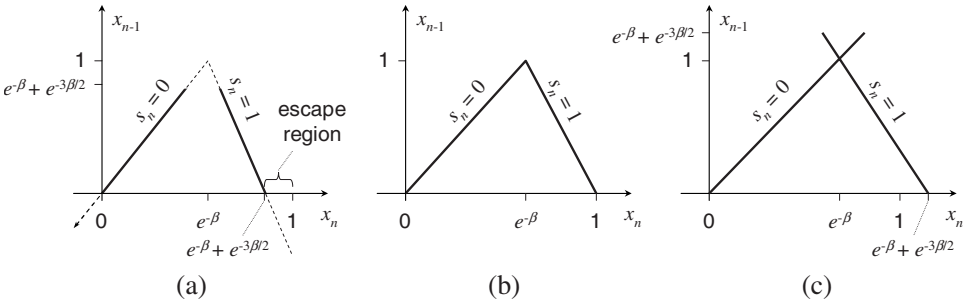

FIG. 3. Reverse-time map for the filter output for (a) strong dissipation $\beta>\tilde{\beta}$, (b) critical dissipation $\beta=\tilde{\beta}$, and (c) weak dissipation $\beta<\tilde{\beta}$.

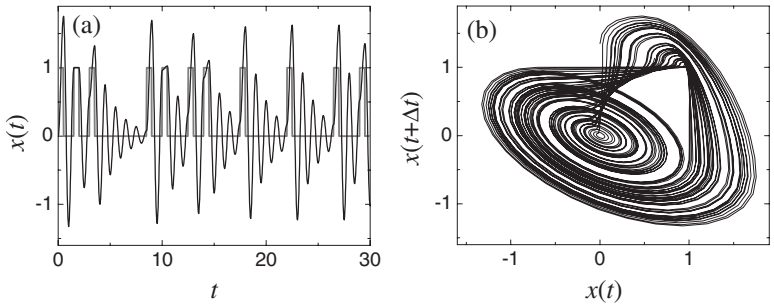

FIG. 4. Sample output from linear filter with matched dissipation $\beta=\tilde{\beta}$: (a) output filter wave form for the input drive signal shown in gray and (b) projection using time-delay embedding ($\Delta t=1/3$).

tor in Rössler's system is characterized by a fractal transverse structure describing an invertible flow.

In this analysis, the critical dissipation $\tilde{\beta}$ was determined by the algebraic condition (8), which set the closed interval for the map (7) to cover the unit interval. A different approach is to match the filter's dissipation—which is the positive Lyapunov exponent for the reverse-time wave form—to the maximum possible entropy for the encoded random source. Assuming p is the probability of the individual symbol $s_n=1$, the entropy of $s(t)$ is

$$h(p) = -\frac{p\ln p + (1-p)\ln(1-p)}{1+p/2} \tag{11}$$

where the numerator is the entropy rate for the random sequence s_n and the denominator is the expected time per symbol. We define a topological source entropy H as the maximum of $h(p)$ over $0 \leqslant p \leqslant 1$. Analysis yields $H=h(\tilde{p})$, where $\tilde{p}$ is the unique real root of $\tilde{p}^3-2\tilde{p}^2+3\tilde{p}-1=0$. This approach yields $\tilde{p}\cong 0.43$ and $H\cong 0.81\ln 2$, which is consistent with the value for $\tilde{\beta}$ found previously via Eq. (8).

We now return to the case of weak dissipation $\beta<\tilde{\beta}$, for which the reverse-time map does not display determinism. In this case, the reduced dissipation of the linear filter is insufficient to accommodate the topological entropy of the random source. We conjecture that determinism can be regained by decreasing the topological source entropy to match the reduced dissipation. A reduced topological entropy implies that certain sequences of random bits are not allowed, which is equivalent to a grammar restriction applied to the bit sequences produced by the random source [9].

We explore this conjecture and verify it for a particular case using a simple grammar restriction. We consider the encoding shown in Fig. 1(b) and a random binary source that is restricted from generating consecutive 0 bits. That is, when the random source outputs a 1 bit, it can follow it with either a 1 or a 0, but whenever the source outputs a 0 bit, it must follow it with a 1. To analyze this source, we need only consider the two random "supersymbols" 1 and 01. Using q and $1-q$ for the probability of the supersymbols 1 and 01, respectively, the topological source entropy is

$$H_r = \max_{0\leqslant q\leqslant 1}\left\{-\frac{q\ln q + (1-q)\ln(1-q)}{5/2-q}\right\}, \tag{12}$$

where the denominator is now the expected time per supersymbol. Calculations provide $H_r\cong 0.51\ln 2$.

In Fig. 5(a), we show the filter output for $\beta=H_r$ and an unconstrained grammar of 0 and 1. A lack of determinism is apparent in the reverse-time return map shown in the inset, which is consistent with analysis for $\beta<\tilde{\beta}$. In Fig. 5(b), we show comparable results for the same filter driven by a random sequence of the supersymbols 1 and 01. We see that applying this grammar restriction has restored determinism to the reverse-time map.

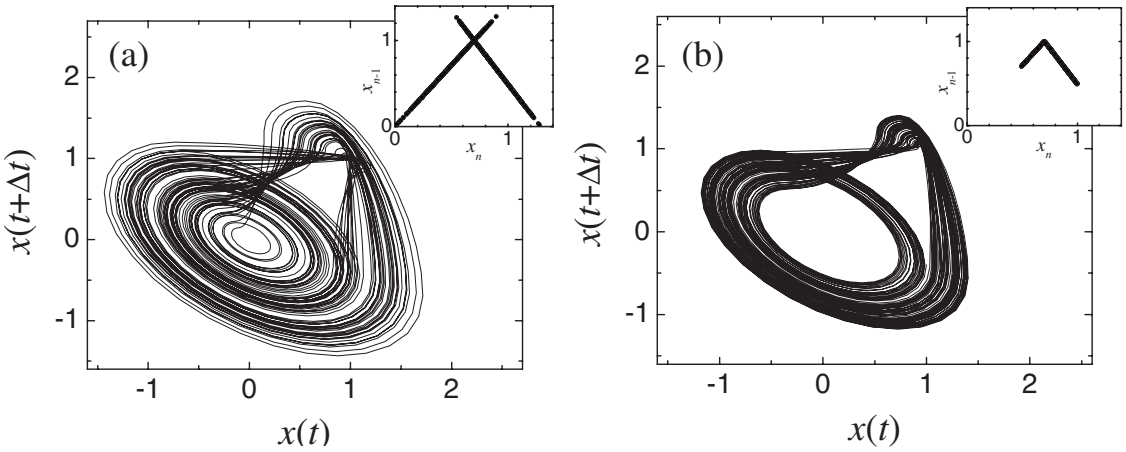

FIG. 5. Time-delay embedding ($\Delta t=1/3$) of the filter output for the folded band encoding with weak dissipation ($\beta=0.511\ln 2$) for (a) an unconstrained random drive and (b) a constrained random drive with topological source entropy matched to the filter dissipation. The insets show the corresponding reverse-time return maps.

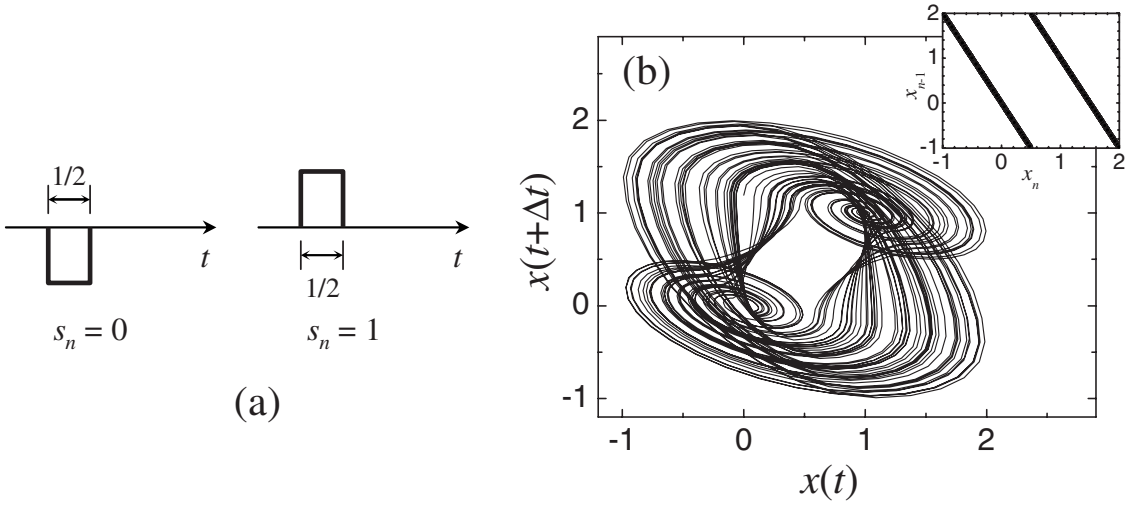

FIG. 6. (a) Encoding of random source used to generate a chaotic set containing both butterfly and folded band dynamics. (b) Sample filter output projected using time-delay embedding ($\Delta t = 1/3$), with inset showing the wave form return map.

The chaotic sets shown in Fig. 2 were generated using the two different encodings shown in Fig. 1. These basis pulses can themselves be viewed as a grammar restriction applied to the more general encoding shown in Fig. 6(a). In this encoding, the two symbols are simply high and low pulses with one-half time unit duration. Using this basis, the butterfly encoding in Fig. 1(a) can be constructed using the supersymbols 00 and 11, while the folded band encoding in Fig. 1(b) is obtained with 00 and 100.

For an unconstrained grammar of the encoding shown in Fig. 6(a), the source entropy is two bits per time unit; thus, we use $\beta = 2 \ln 2$ to view the fully developed chaotic set for this encoding. The resulting "attractor" obtained by time-delay embedding is shown in Fig. 6(b), and the inset shows the return map for the filter output sampled at the end of each applied pulse. The reverse-time map shows determinism and a positive Lyapunov exponent, indicating the reverse-time wave form is chaotic. The geometric structure shown in Fig. 6(b) contains within it both butterfly and folded band dynamics, as well as any other chaotic sets due to different grammar restrictions of the base encoding shown in Fig. 6(a).

In conclusion, we have shown that the linear synthesis of chaotic wave forms is not restricted to the singular case of a Lorenz-like butterfly topology. We have shown that the same linear filter that generates reverse-time, Lorenz-like chaotic wave forms can yield a folded band topology when excited using a different encoding of the random source. We exposed the interplay of filter dissipation, reverse-time Lyapunov exponents, determinism, and the topological entropy of the drive. We also used the filter to construct a topological structure that contains both the butterfly and folded band topologies. This chaotic set suggests that an attractor might be realized that encompasses both of these fundamental paradigms of nonlinear dynamics.

[1] S. T. Hayes, in Applied Symbolic Dynamics, SIAM Conference on Applications of Dynamical Systems, Snowbird, UT, 2003 (unpublished).
[2] S. T. Hayes, J. Phys.: Conf. Ser. **23**, 215 (2005).
[3] Y. Hirata and K. Judd, Chaos **15**, 033102 (2005).
[4] N. J. Corron, S. T. Hayes, S. D. Pethel, and J. N. Blakely, Phys. Rev. Lett. **97**, 024101 (2006).
[5] E. N. Lorenz, J. Atmos. Sci. **20**, 130 (1963).
[6] O. E. Rössler, Phys. Lett. **57A**, 397 (1976).
[7] E. Ott, *Chaos in Dynamical Systems* (Cambridge University Press, Cambridge, U.K., 1993).
[8] P. Collet and J. P. Eckmann, *Iterated Maps of the Interval as Dynamical Systems* (Birkhäuser, Boston, 1980).
[9] S. Hayes, C. Grebogi, and E. Ott, Phys. Rev. Lett. **70**, 3031 (1993).